

Near-infrared observations of dusty white dwarfs

Laura K. Rogers¹ , Siyi Xu², Amy Bonsor¹, Simon Hodgkin¹,
Kate Y. L. Su³, Ted von Hippel⁴ and Michael Jura[†]

¹Institute of Astronomy, University of Cambridge, Madingley Rd, Cambridge, CB3 0HA, UK
email: laura.rogers@ast.cam.ac.uk

²Gemini Observatory, 670 N. A'ohoku Place, Hilo, HI 96720, USA

³Steward Observatory, University of Arizona, 933 N Cherry Avenue, Tucson, AZ 85721, USA

⁴Department of Physical Sciences, Embry-Riddle Aeronautical University, Daytona Beach, FL 32114, USA

Abstract. Planetary material in the atmospheres of white dwarfs is thought to be scattered inwards from outer planetary systems. Dusty emission in the infrared traces the accretion. As the scattering of many small asteroids is a stochastic process, variability in the infrared emission is predicted. We report a 3 year near-infrared (*J*, *H* and *K*) monitoring campaign of 34 dusty, polluted white dwarfs which aims to search for dust emission variability. We find all white dwarfs have consistent near-infrared fluxes, implying the excess emission is stable. This suggests tidal disruption events which lead to large variabilities are rare and quick (< 1 year) and become stable within a few years. For WD 0408–041, the system that shows both increases and decreases in dust emission over 11 years, our *K* band data suggest a potential colour change associated with the dust emission that needs further confirmation.

Keywords. white dwarfs, planetary systems, minor planets, asteroids

1. Introduction

Planetary material is found to survive to the white dwarf phase. Observations suggest that between 25% and 50% of white dwarfs have atmospheric pollution of elements heavier than helium (Zuckerman *et al.* 2003, 2010; Koester *et al.* 2014). The rapid gravitational settling times in comparison to the white dwarfs' cooling age implies ongoing accretion from a circumstellar reservoir.

The driving mechanism that results in atmospheric pollution is debated. The favoured theory cites outer planets which perturb asteroids towards the Roche radius of the white dwarf, where they become tidally disrupted, sublimate, and subsequently accrete on to the atmosphere of the white dwarf (Debes & Sigurdsson 2002; Jura *et al.* 2003; Farihi *et al.* 2010; Veras *et al.* 2014). This theory is supported by the discovery of disintegrating planetesimals transiting the polluted and dusty white dwarf WD 1145+017, and the white dwarf ZTF J013906.17+524536.89 (Vanderburg *et al.* 2015; Vanderbosch *et al.* 2019).

G29-38 was the first polluted white dwarf to be discovered to also display an infrared excess (Zuckerman & Becklin 1987). Follow-up observations confirmed its dusty nature (Graham *et al.* 1990). To date, around 40 polluted white dwarfs have a *Spitzer* confirmed infrared excess; this is calculated as between 1.5% and 4% of white dwarfs (e.g. Becklin *et al.* 2005; Kilic *et al.* 2006; Jura *et al.* 2007; Rebassa-Mansergas *et al.* 2019;

† Deceased

Wilson *et al.* 2019). Eight of the white dwarfs with dust also show evidence of circumstellar gas in emission near the same orbital distance as the dust (e.g. Gänsicke *et al.* 2006).

The scattering of planetary bodies that lead to the atmospheric pollution is expected to be a stochastic process (Wyatt *et al.* 2014), with variability predicted on human timescales. Variability in the dusty emission is seen for a few white dwarfs. The white dwarfs SDSS J095904.69–020047.6 (hereafter WD J0959–0200) and SDSS J122859.92+104033.0 (WD 1226+110) demonstrated large drops in dust flux (Xu & Jura 2014; Xu *et al.* 2018), whilst WD 0408–041 (GD56) among others show both increases and decreases in the flux (Farihi *et al.* 2018; Swan *et al.* 2019). The first white dwarf discovered with dust variability was WD J0959–0200. The 3–5 μm flux dropped by 35% between observations separated by a year, and the near-infrared K band flux dropped by 18.5% between observations separated by 8 years (Xu & Jura 2014). The large K band excess for this white dwarf means the dust is hot and close in. The mid-infrared flux drop occurred within a year, implying the variability event was large and became stable quickly.

2. Observations

Motivated by the large infrared variability in WD J0959–0200, we present a study to search for near-infrared variability in 34 dusty white dwarfs. We aim to characterise how the sample varies in the near-infrared in order to better understand how dusty material arrives in the atmospheres of the white dwarfs. We use the Wide Field Camera (WFCAM) on the UK Infrared Telescope (UKIRT) on Mauna Kea, Hawaii. We obtain J , H and K band photometry of our white dwarfs up to 6 times over the 3 year monitoring campaign. We probe short timescales (minutes) between individual frames taken on an observation date, and long timescales (years) between observation dates.

All data obtained with WFCAM were pipeline-processed by the Cambridge Astronomical Survey Unit using standard infrared photometry data reduction steps (CASU, Irwin *et al.* 2004; Dye *et al.* 2006). Further processing using the LIGHTCURVES software[†] was executed to photometrically calibrate the light curves (Irwin *et al.* 2007).

At each observation date, a number of observations were taken depending on the magnitude of the white dwarf. In order to robustly study the statistics of the photometry, the same analysis method was applied to all dusty white dwarf observations regardless of the magnitude and the number of measurements in the J , H and K bands. Gaussians were fitted to the distribution of photometrically corrected magnitudes from the LIGHTCURVES software. A Markov Chain Monte Carlo approach was implemented to model the magnitude distribution with a Gaussian, from this the mean and standard deviation were inferred. Please see Rogers *et al.* (submitted) for further details.

To ensure that any variability detected was real, background stellar objects were analysed using the same approach for comparison. The wide field of view of WFCAM ensures many background stars are present in the data. The results for the background objects give us a base to determine the observation sensitivity to detecting variability.

3. Results

3.1. K band variability

Of the near-infrared bands, the K band is the most sensitive to the dust, therefore, this is where we probe variability. Fig. 1 plots the median value of the magnitude and standard deviation from the Gaussian fit for the white dwarfs and background stars in the K band. All white dwarfs have standard deviations which are consistent with the background stellar objects within 2σ . We conclude that from our survey all our objects

[†] <https://github.com/mdwarfgeek/lightcurves>

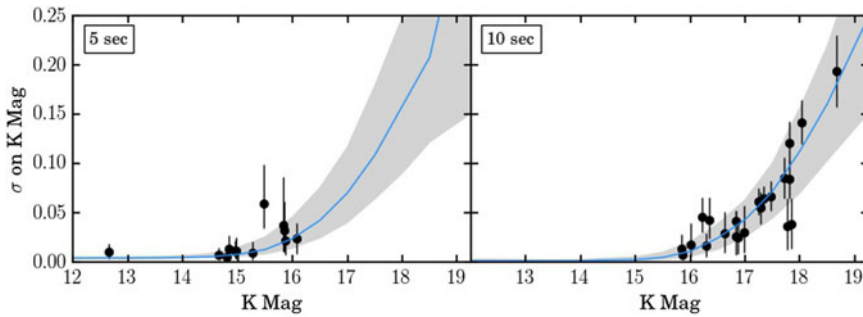


Figure 1. The median K magnitude against the median standard deviation on this magnitude for white dwarfs and background stars in the UKIRT survey. Due to differing observing strategies, the white dwarfs observed with 5 and 10 second frames were analysed separately. The background stars are given by the blue median line, with the 16th and 84th percentile confidence levels for objects in bins of width 0.5 mag. This represents the sensitivity of the survey as a function of magnitude. The white dwarfs are plotted in black with the errors as the 16th and 84th percentiles. This plot is used to distinguish white dwarfs which are variable from those that follow the background distribution.

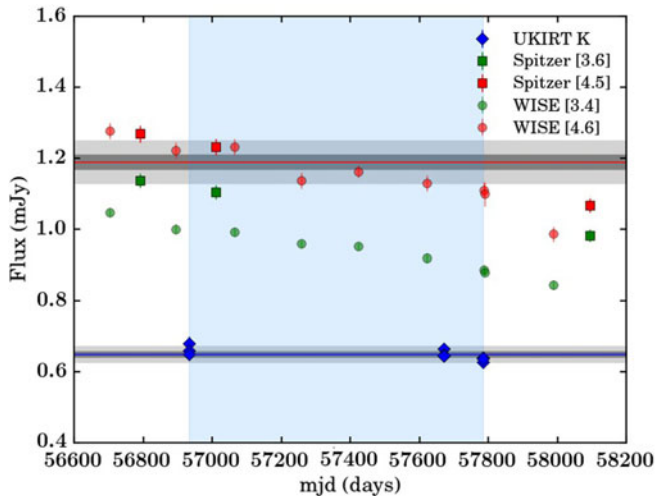


Figure 2. WD 0408–041 light curve of the UKIRT K band data and the *Spitzer*/*WISE* data where [Farihi et al. \(2018\)](#) observed a drop in the mid-infrared flux. The grey regions represent the 1 and 3 σ median variability constraint for the K band, scaled up to *Spitzer* wavelengths (assuming a constant colour temperature). The blue region shows the period of time that we have UKIRT observations. Figure adapted from [Farihi et al. \(2018\)](#).

have stable K band contributions to the dust. This may imply that the tidal disruption events which lead to large variabilities are rare and occur quickly (< 1 year), then once they occur they become stable within a few years.

3.2. WD 0408–041

WD 0408–041 has previously shown dust variation at 3–5 μm demonstrating brightening and dimming with peak-to-peak changes of 20% over 11.2 yrs ([Farihi et al. 2018](#)); a four year data set is shown in Fig. 2. We use the UKIRT K band standard deviation to predict the expected variability at 4.5 μm by assuming the dust emission has a constant colour temperature (i.e., the change is due to the amount of dust, not the location, see

Rogers *et al.* (submitted) for further details). The shaded grey regions in Fig. 2 show the variability constraint for the K band, and the predicted variability constraint at $4.5\ \mu\text{m}$. As WD 0408–041 has a large K band excess, variability observed at mid-infrared wavelengths should be mimicked at a lower level in the K band, unless there is a colour change associated with the flux change.

Over the length of the UKIRT survey (blue shaded region in Fig. 2), the change in *Spitzer* $4.5\ \mu\text{m}$ flux is consistent with the variability constraint derived from the K band, implying that during the three year survey there is no colour change associated with the variability. However, considering the four year baseline, even at 3σ , the *Spitzer* fluxes lie outside of the grey shaded region. The most significant drop in *Spitzer* flux is around 58100 days. We do not have simultaneous K band observations, with the closest K band measurement being over a year previous to this. There is previous evidence that large scale changes can occur on time-scales of less than a year (Xu & Jura 2014), so changes can be large and occur quickly. We conclude that a further K band measurement is required to understand whether the K band flux also dropped around 58100 days, or if there is a colour change associated with this variability. If the latter is true, it may explain why the K band appears to be stable for all objects in the UKIRT monitoring campaign.

References

- Becklin, E. E., Farihi, J., Jura, M., Song, I., *et al.* 2005, *ApJL*, 632, 119
- Debes, J. H. & Sigurdsson, S. 2002, *ApJ*, 572, 556
- Dye, S., Warren, S. J., Hambly, N. C., Cross, N. J. G., *et al.* 2006, *MNRAS*, 372, 1227–1252
- Farihi, J., Barstow, M. A., Redfield, S., Dufour, P., *et al.* 2010, *MNRAS*, 404, 2123–2135
- Farihi, J., van Lieshout, R., Cauley, P. W., Dennihy, E., *et al.* 2018, *MNRAS*, 481, 2601–2611
- Gänsicke, B. T., Marsh, T. R., Southworth, J., & Rebassa-Mansergas, A. 2006, *Science*, 314, 1908–1910
- Graham, J. R., Matthews, K., Neugebauer, G., & Soifer, B. T. 1990, *ApJ*, 357, 216–223
- Irwin, M. J., Lewis, J., Hodgkin, S., Bunclark, P., *et al.* 2004, *International Society for Optics and Photonics*, 5493, 411–422
- Irwin, J., Hodgkin, S., Aigrain, S., Hebb, L., *et al.* 2007, *MNRAS*, 377, 741–758
- Jura, M. 2003, *ApJL*, 584, 91
- Jura, M., Farihi, J., & Zuckerman, B. 2007, *ApJ*, 663, 1285
- Kilic, M., von Hippel, T., Leggett, S. K., & Winget, D. E. 2006, *ApJ*, 646, 474
- Koester, D., Gänsicke, B. T., & Farihi, J. 2014, *A&A*, 566, A34
- Rebassa-Mansergas, A., Solano, E., Xu, S., Rodrigo, C., *et al.* 2019, *MNRAS*, 489, 3990–4000
- Swan, A., Farihi, J., & Wilson, T. G. 2019, *MNRAS: Letters*, 484, 109–113
- Vanderburg, A., Johnson, J. A., Rappaport, S., Bieryla, A., *et al.* 2015, *Nature*, 526, 546
- Vanderbosch, Z., Hermes, J. J., Dennihy, E., Dunlap, B. H., *et al.* 2019, [arXiv:1908.09839](https://arxiv.org/abs/1908.09839)
- Veras, D., Leinhardt, Z. M., Bonsor, A., & Gänsicke, B. T. 2014, *MNRAS*, 445, 2244–2255
- Wilson, T. G., Farihi, J., Gänsicke, B. T., & Swan, A. 2019, *MNRAS*, 487, 133–146
- Wyatt, M. C., Farihi, J., Pringle, J. E., & Bonsor, A. 2014, *MNRAS*, 439, 3371–3391
- Xu, S. & Jura, M. 2014, *ApJL*, 792, 39
- Xu, S., Su, K. Y., Rogers, L. K., Bonsor, A., *et al.* 2018, *ApJ*, 866, 108
- Zuckerman, B. & Becklin, E. E. 1987, *Nature*, 330, 138
- Zuckerman, B., Koester, D., Reid, I. N., & Hüensch, M. 2003, *ApJ*, 596, 477
- Zuckerman, B., Melis, C., Klein, B., Koester, D., *et al.* 2010, *ApJ*, 722, 725